High-Efficiency Broadband Polarization-Independent Superscatterer Using Conformal Metasurfaces

He-Xiu Xu* [1, 2], ChengWei, Qiu[1], and Lianlin Li[3], Chun Sun[2], Shiwei Tang[4]
(1) Department of Electrical and Computer Engineering, National University of Singapore, Singapore 117583, Singapore
(2) Air and Missile Defense College, Air force Engineering University, Xi'an 710051, China
(3) School of Electronic Engineering and Computer Sciences, Peking University, Beijing 100871, China
(4) Department of Physics, Faculty of Science, Ningbo University, Ningbo 315211, China

Abstract

A sophisticated strategy to design a metasurface wrapping over arbitrarily shaped objects is proposed, where optical aberrations are commonly introduced. By designing each meta-atom with required position and phase compensation, exact EM wavefronts are restored. For verification, several conformal metasurfaces were designed and numerically studied on metallic cylinders at microwave spectrum. One proof-of-concept device is fabricated, and experimentally characterized. All results have demonstrated the desirable dual-beam superscatterer with strong backscattering enhancement toward two directions, indicating that the distortions induced by arbitrary platform can be efficiently corrected. Our method lay a solid platform for designing high-performance multifunctional optoelectronic devices equipped on high-speed vehicles and aircrafts.

1. Introduction

Curved platform with arbitrary packaging and shape are commonly available in practice. This is especially true for the high-speed aircrafts, missiles and vehicles, where aerodynamics and aesthetics are a major concern. Moreover, multi-faced or curved structure are also highly preferably and utilized in stealth applications due to its low bistatic scattering. As a consequence, there is an extensive research and interest toward conformal techniques and array antennas in last decades [1,**Error! Reference source not found.**]. Among them, the conformal design to improve scattering of a curved object is rarely seen since most work is confined to radar cross section (RCS) reduction [2]. Moreover, a superscatterer with flexible beam number and beam steering on curved structure is exclusively vital to improve survivability, rescue or navigation safety of friendly high-speed target in remote areas [3]. Therein, we also expect that the detected signal can be safely achieved for emitting wave of any polarization.

Metasurface, composed of a set of planar subwavelength meta-atoms [4-10], has recently attracted enormous interest in manipulating electromagnetic (EM) waves by science and engineering community. Since abrupt phase discontinuities were utilized, it is not necessary to employ thick materials to accumulate the required phase. Such feature enables the metasurface superthin, flexible, low loss, and easily fabricated, advancing a big step toward real applications. Despite fruitful progress toward planar design, few is aimed on an arbitrary platform with large curvature [9]. Moreover, available conformal designs suffer from narrow bandwidth and rigorous polarization restriction, which hinders it back from real-world applicability.

Here, we introduced a sophisticated strategy inspired from ray-tracing technique, aiming to fill above gap. As a demonstration, the metasurface is designed to wrap over a metallic cylinder for easy design. To facilitate the desired polarization-independent EM response, the Pancharatnam–Berry (PB) metasurface [7] is utilized to generate the high-efficiency superscattering behavior. Therein, the polarization sensitivity of measurface's functionality can be released since any linearly polarized (LP) wave can be decoupled as a linear combination of two circularly polarized (CP) waves of different handness. Two inverse linear-phase gradients are symmetrically formed about the axes of the metallic cylinder to yield a pair of symmetric highly-directive beams along two opposite directions. The key to the high-efficiency superscattering is that the phase error induced by the curvature is compensated and minimized point by point and thus planar uniform wavefronts are restored at predicted directions.

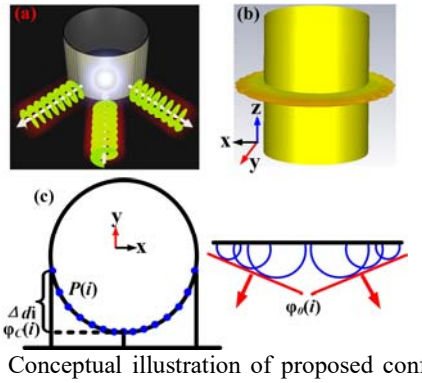

Figure 1. Conceptual illustration of proposed conformal metasurface. (a) Schematic functionality under the illumination of a CP wave or a LP wave with arbitrary polarization. (b) Typical scattering pattern of a metallic

cylinder. (c) Phase compensation inspired by ray-tracing approach to restore two symmetric planar wavefronts.

2. Fundamentals, Theory and Design

The basic principle behind the dual-beam superscatterer lies in generalized Snell's law [4] see the conceptual function illustration shown in Fig. 1(a). Two highly-directive scattering beams are obviously inspected across the horizontal plane when our designed metasurface is wrapped over a cylinder. However, as portrayed in Fig. 1(b), a doughnut-like scattering pattern with almost homogenous intensity is expected across half circumference of azimuth ϕ (illumination region) for the bare cylinder. The superthin metasurface modulates the wavefronts of a metallic cylinder, facilitating the homogenous scattering energy to be collected and concentrated to two arbitrary angles. To modulate the EM wave without distortion on arbitrary platforms in reflection scheme, we first project the flexible surface to a common reference plane by calculating the optical path difference $\varphi_C(i)$ at each point i according to ray optics approximation and then obtain the required phase distribution $\varphi_0(i)$ based on the functionality we want to achieve on the plane, see Fig. 1(c). The physics can be also understood as that $\varphi_0(i)$ determines the functionality while $\varphi_C(i)$ modifies the phase error induced during non-planar packaging.

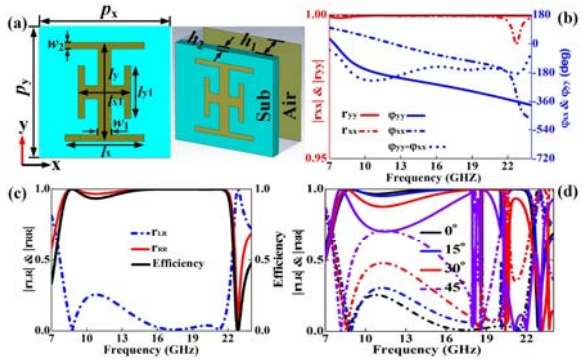

Figure 2. Topology and EM property of the broadband PB meta-atom. (a) Element structure. EM response under illumination of (b) x/y-polarized LP wave, and CP wave of (c) normal and (d) oblique incidence. The geometrical parameters are optimized and detailed as l_x=6, l_y=7.5, l_{x1}=3.8, l_{y1}=2, w_1=1, w_2=0.5, h_1=0.06 and h_2=4 mm. l_x=6, l_y=7.5, l_{x1}=4, l_{y1}=4, w_1=1, w_2=0.5, h_1=0.06 and h_2=4 mm.

For convenience and easy design, the inversely symmetric phase gradients are designed only along circumference and those along axial and radial direction are left constant. To guarantee the linear phase profile, the position of the i^{th} element starting from one specified point (original point) should fulfill $P(i) = R_0 \arcsin((i-1)p/R_0)$ and their initial phases are progressively increased with $\varphi_0(i+1) - \varphi_0(i)$ =90°, $i = 1, 2, ..., n$. Here p is the lattice constant of the meta-atoms, R_0 is radius of the cylinder and n is the number of elements utilized for shaping each high-efficiency beam. Therein, each meta-atom is still periodically arranged when they are projected to the reference plane. Then, the imparted phase utilized to correct the distortions induced by curved shape at f_0 is determined by considering the optical path difference

$$\begin{aligned}\varphi_C(i) &= k_0 * 2\Delta di \\ &= 4\pi R_o / \lambda_0 * [1 - \cos(\arcsin((i-1)p/R_o))]\end{aligned} \quad (1).$$

As a consequence, the phase shift imposed by the metasurface should be $\varphi(i) = \varphi_0(i) + \varphi_C(i)$. Using this design procedure, arbitrary function can be exactly realized by the flexible conformal metasurface.

Now that the physics and strategy is clear, the next step lies in the design of meta-atoms to map the determined phase distribution. To achieve a broad operation bandwidth, rotational metallic Jerusalem cross with PB phase is utilized, see Fig. 2(a). The meta-atom is composed of a dielectric layer, an air spacer and a backed metallic ground. The Jerusalem cross is etched on top of the dielectric layer with dielectric constant of ε_r=3.4 and thickness of 0.06 mm, while the air layer is utilized to enhance the bandwidth. The criterion of φ_{yy}-φ_{xx}=180° is utilized to guarantee the near-unity CP conversion efficiency by suppressing any component that does not carry PB phase information. Here, we employ the engineering method [10] to enable the slope of φ_{yy} and φ_{xx} to be almost parallel within a broad bandwidth by modulating the length of three orthogonal bars of both "H" structures. After cautious optimizations, we achieve φ_{yy}-φ_{xx}=180°±45° within 8.3~23.5 GHz in Fig. 2(b), corresponding to a fractional bandwidth of 95.6%. Moreover, the reflection magnitude remains almost unity across the entire band, which is necessary for high-efficiency superscatterer. As expected in Fig. 2(c), the CP copolarization conversion efficiency is more than 93.5% across 8.17~22.1 GHz where the cross-polarization component (less than 0.25) is almost suppressed. Finally, the EM response under the oblique illumination is depicted in Fig. 2(d). We can see that the efficiency and bandwidth (shifted high-edge frequency downward) are progressively worsened when the incidence arises from 0° to 45° in terms of 15°. Despite this, a desirable efficiency of more than 87.7% is achieved when θ approaches 30° and it is still better than 70.5% even for θ=45°. Such feature is very important for conformal design on arbitrary platforms, where the meta-atoms with large curvature are typically illuminated obliquely.

By progressively rotating above meta-atoms with Φ , we can achieve a PB phase of $\varphi = 2\Phi$ under CP wave excitation. As a consequence, the imposed correctional phase calculated by Eq. (1) can be realized just by rotating aforementioned meta-atoms with appropriate Φ at predicted positions. Then the superscatterer can be engineered by wrapping the flexible conformal metasurface over conductor cylinder.

As a proof of the principle, we first employ a total of 21 dipoles mounted on the cylindrical surface with R_0=99.06 mm to mimic a conformal metasurface, see Fig. 3(a).

Each dipole is distributed with progressively enlarged distance along the circumference and is fed with identical amplitude but specific phase determined by above procedure at 12 GHz. In such case, effect of scattering amplitude loss (distortion) induced by curvature can be avoided. Due to the shielding effect, one half circle of 21 dipoles is necessary. Different from the scattering scenario, we require $\varphi(i)=\varphi_0(i)+\varphi_C(i)/2$ to shape the radiation wave to desired directions since no illumination phase error is induced. For comprehensive study, three dipole arrays are considered on the same curved platform and the corresponding phases are portrayed in Fig. 3(b). The first dipole array is designed with two beams directed at constant $\phi=\pm45^o$ and f_0, the phase tolerance is compensated and minimized point by point based on following equation.

$$\varphi(i)=2\sqrt{2}\pi R_o/\lambda_0\,[1-\cos(\phi_0-\arcsin((i-1)p/R_o))] \\ *\sin(\phi_0-\arcsin((i-1)p/R_o)) \quad (2)$$

The latter two dipole arrays are equipped using linear phase with (case 2) and without (case 3) phase compensation for curvature.

As expected in Fig. 3(c) and 3(d), very desirable radiation patterns are clearly observed within 6~18 GHz, i.e., two symmetric radiation beams with enhanced intensity directed toward $\phi=\pm45^o$ in case 1 while two high-efficiency anomalous beams steered at $\phi=\pm\sin^{-1}(\lambda/Np)$ with specular radiation almost suppressed in case 2. The highly-concentrated beam steered from 69.6° at 8 GHz to 24.6° at 18 GHz. The slightly enhanced specular radiation and distorted beam angle at low frequencies is attributable to the reduced electrical array aperture where ray-tracing approximation introduces some tolerances. Nevertheless, this does not pose any effect on the verification of our compensation strategy. Such declaration finds strong support from the almost completely deteriorative radiations (emanative radiations with dispersive intensity) in case 3, see Fig. 3(e). It is even hardly to see a clear beam, and instead the power intensity is discretized toward numerous directions without phase correction, illustrating the effectiveness of our approach.

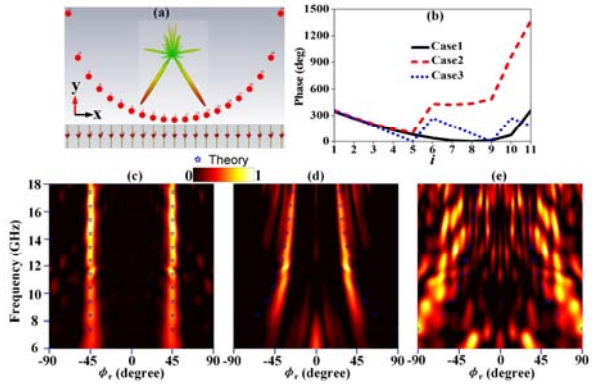

Figure 3. Numerical characterization of three dipole arrays each forming half of a circle with R_0=99.06 mm to mimic a conformal metasurface. The radiation/scattering intensity at each frequency is first normalized to the total energy across the entire illumination region ($\overline{P}(\phi_r,f_i)=P(\phi_r,f_i)/\sum_{\phi_r=-90}^{\phi_r=90}P(\phi_r,f_i)$) and then normalized to the maximum intensity $\max(\overline{P}(\phi_r,f_i))$. Three dipole arrays are considered: directional radiation at $\phi=\pm45^o$ (case 1), high-efficiency anomalous radiation at $\phi=\pm\sin^{-1}(\lambda/Np)$ (case 2), and deteriorative radiation (case 3). In case 1 and case 2 the phases are exactly designed, whereas in case 3 there is no phase correction. (a) Topology of the dipole array, the inset shows the typical 3D radiation pattern in case 2. (b) Corresponding exciting phases of each dipole in three cases. Far-field radiation power intensity of three dipole arrays in (c) case 1, (d) case 2 and (e) case 3.

3. Numerical and Experimental Results

We now further evaluate the performance of our conformal metasurfaces by replacing the dipoles with real PB meta-atoms. For verification, we have designed and fabricated a proof-of-concept sample wrapping on a cylinder of R_0=95 and h=250 mm. Since available CP horns in laboratory operate within 6~18 GHz, we design another meta-atom target at that band, see Fig. 4. As can be seen, two high-efficiency scattering patterns are clear seen. This is in sharp contrast with the bare cylinder, where the scattering is almost homogenous across the circumference. The total scattering by the metasurface-coated cylinders is very close to that of flat conducting plate with the same projected size. The operation band with precise steering angle shifts as f_0 for conformal metasurface. However, almost identical beam direction is achieved between theory and numerical calculation for planar metasurface. Moreover, the beam is narrowed when R_0 increases from 95 to 156 mm due to the contribution of array factor. As to the bare cylinder, the specular scattering enhances progressively as frequency ascends and finally dominates the energy across the azimuth like a planar metallic plate. This is because at high frequency the curved surface can be approximated as a plane.

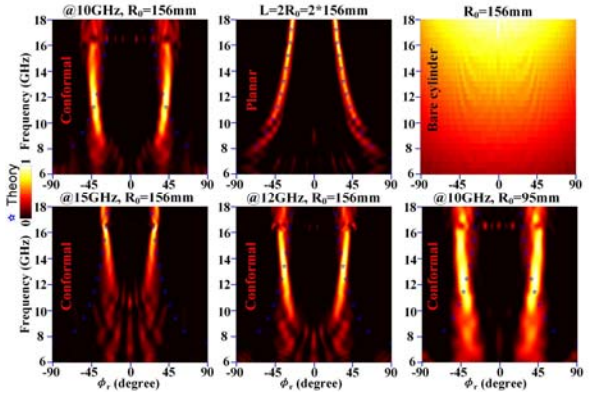

Figure 4. Numerical characterization of conformal metasurfaces on cylinders of R_0=156 and R_0=95 mm. The

geometrical parameters of utilized basic meta-atom are detailed as l_x=6, l_y=7.5, l_{x1}=4, l_{y1}=4, w_1=1, w_2=0.5, h_1=0.06 and h_2=4 mm. The conformal metasurface is designed at different f_0 of 10, 12 and 15 GHz.

Fig. 5(a) portrays the photograph of the fabricated flexible sample with a planar area of $L*h=\pi*95*250$ mm^2. In fabrication, we first attach a double-faced cardboard with ε_r=1 and thickness of 4 mm on the metallic cylinder, and then stick the superthin film to the cardboard. The sample was then characterized in a microwave anechoic chamber using an angle-resolved bistatic scattering experimental setup, also see Fig. 5(a). As shown in Fig. 5(b), very well-defined dual beams can be clearly examined ranging from 8 to 18 GHz. However, the cross-polarized scattering normalized to the co-polarized one is negligible within 8~17 GHz, see Fig. 5(c), revealing a high conversion efficiency thanks to the preserved φ_{yy}-φ_{xx}=180º. Therefore, we obtain a high efficiency of ~82% (90.3%) in measurement (simulation) across 8~18 GHz, see Fig. 5(d). Such highly concentrated scattering for curved surface is very desirable with respect to the bare cylinder, where the reflection is almost averaged across the azimuth.

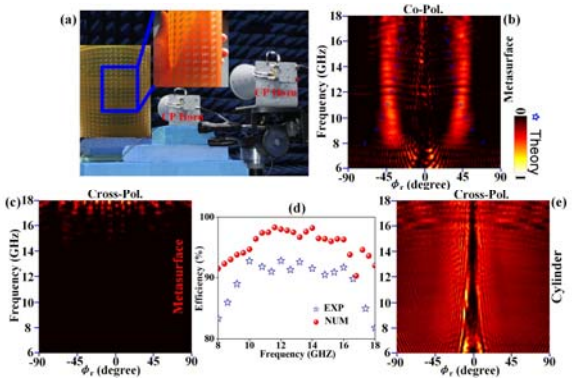

Figure 5. Experimental characterization of conformal metasurface wrapping on the cylinder of R_0=95 mm. (a) Photograph of the fabricated sample and angle-resolved bistatic RCS measurement setup. (b) Copolarized and (c) cross-polarized scattering component of the superscatterer. (d) Comparison of efficiency between experiments and numerical calculations. (e) Cross-polarized scattering intensity of the bare metallic cylinder.

4. Conclusions

To sum up, we have proposed and verified a general method to design flexible high-efficiency superscatterer exhibiting desired broadband performances in analogue to their planar counterparts. In this regard, the geometrical form can be decoupled from its EM function, which enables the metasurface to be equipped among any shaped non-planar platforms and stringent packaging. For verification, a set of conformal metasurfaces are designed at microwave frequency by modulating the non-dispersive PB phase. Dual planar wave with minimized wavefront error are recovered at two predicted angles since perfect phase profile is restored at each point of curved surfaces using ray-tracing technique. Theoretical, numerical and experimental results coincide well, showing that the measured (simulated) efficiency of anomalous reflection can be approached above 82% (90.3%) within 8~18 GHz. Our strategy, low profile and flexible, affords a possible avenue to generate EM superscattering of any curved surface with versatile beam number and beam angle without polarization consideration.

5. Acknowledgements

This work was supported by National Natural Science Foundation of China under Grant Nos. 61501499, National Defense Foundation of China under Grant No. 2201078, Key Program of National Natural Science Foundation of Shaanxi Province under Grant No. 2017KJXX-24, Natural Science Foundation of Shaanxi Province under Grant No. 2016JQ6001, China Scholarship Fund (CSC) under Grant No. 20173059 and also Aviation Science Foundation of China under Grant No. 20161996009.

6. References

1. L. Josefsson and P. Persson, Conformal array antenna theory and design. Piscataway, NJ: IEEE Press, 2006.
2. H.-X. Xu, S. Ma, X. Ling, X.-K. Zhang, S. Tang, T. Cai, S. Sun, Q. He, L. Zhou, "Deterministic approach to achieve broadband polarization-independent diffusive scatterings based on metasurfaces," *ACS Photonics*, 2017, DOI: 10.1021/acsphotonics.7b01036.
3. H.-X. Xu, G.-M. Wang, K. Ma, and T. J. Cui, "Superscatterer illusions without using complementary media," *Adv. Opt. Mater.*, **2**, 2014, pp. 572-580.
4. N.F.Yu, P. Genevet, M.A.Kats, et al. "Light propagation with phase discontinuities: generalized laws of reflection and refraction," *Science*, **334**, 2011, pp. 333-337.
5. X. Zhang, Z. Tian, W. Yue, J. Gu, S. Zhang, J. Han, et al., "Broadband terahertz wave deflection based on c-shape complex metamaterials with phase discontinuities," *Advanced Materials*, **25**, 2013, pp. 4567-4572.
6. F. Aieta, M. A. Kats, P. Genevet, and F. Capasso, "Multiwavelength achromatic metasurfaces by dispersive phase compensation," *Science*, **347**, 2015, pp. 1342-1345.
7. W. Luo, S. Xiao, Q. He, S. Sun, L. Zhou, "Photonic spin hall effect with nearly 100% efficiency," *Adv. Opt. Mater.* **3**, 2015, pp. 1102-1108.
8. L. Li, T. J. Cui, W. Ji, S. Liu, J. Ding, X. Wan,Y. B. Li, M. Jiang, C.-W. Qiu & S. Zhang, "Electromagnetic reprogrammable codingmetasurface holograms," *Nat. Commun.*, **8**, 2017, p. 197.
9. X. Ni, Z. J. Wong, M. Mrejen, Y. Wang, X. Zhang, "An ultrathin invisibility skin cloak for visible light," *Science*, **349**, 2015, pp. 1310-1314.
10. H.-X. Xu, S. Sun, S. Tang, S. Ma, Q. He, G.-M. Wang, T. Cai, H.-P. Li, and L. Zhou, "Dynamical control on helicity of electromagnetic waves by tunable metasurfaces," *Scientific Reports*, **6**, 2016, p. 27503.